Estimation of Flight and Geometry Parameters for low-Boom Aircraft Design using the Unscented Kalman Filter

Ioanna Anagnostaki[1], Petros Nikolaou[2]

[1] Department of Physics, University of Patras, Patras, Greece
[2] Department of Mechanical Engineering and Aeronautics, University of Patras, Patras, Greece

Abstract

In this work the flight characteristics and aircraft geometry required to produce a certain sonic boom signature are estimated using the Unscented Kalman filter (UKF). The Kalman filter is an algorithm that estimates state spaces by combining model predictions and observational data. The UKF extends the Kalman filter to nonlinear systems. Instead of linearizing the system, it uses sampling points (sigma points) to capture the mean and covariance of the state distribution. For the calculations the UKF requires a state vector xk , a measurement vector zk, and a mathematical model. Initially, sigma points are calculated by the mean of the state vector and its covariance. Next a prediction is made using the mathematical model. After that the UKF updates the prediction using the Kalman gain and measurements. The work is organized in two phases. First, UKF is validated by using it to estimate the flight parameters, Mach number and altitude, required by a certain aircraft geometry to achieve measured sonic boom overpressure and duration. Second, UKF is used to solve the inverse design problem where the flight parameters and aircraft shape are estimated so that a target low-boom signature is produced. For the first phase the state vector includes flight parameters. For the second phase the shape and lift of the aircraft are included. The measurement vector includes sonic boom overpressure and duration in both phases. Rise time is added for the second phase. Two mathematical models are employed: the Carlson empirical formula and a non-linear propagation model. **Keywords**: Unscented Kalman filter, Sonic Boom, Inverse Aircraft Desing Algorithm.

1. Introduction

The Kalman filter is a powerful algorithm used to track and predict the behavior of dynamic systems by reducing estimation errors. It operates in two main stages: first, it predicts the system's future state, and then it refines this prediction using incoming measurements. Commonly applied in areas such as physics, aeronautics, aeroacoustics and aerospace, it handles uncertainty by combining prior estimates with observed data. Additionally, it can be derived from a maximum likelihood perspective, providing a stronger understanding of its statistical basis.[1][2]

Filtering aims to isolate useful information from a signal while discarding irrelevant components. The effectiveness of a filter is evaluated through a cost (or loss) function, with the objective being to minimize this measure. The filter is named in honor of Rudolf E. Kálmán who in 1960, he published his landmark paper, which introduced a recursive approach to solving the discrete-data linear filtering problem Kalman, so Kalman filtering is an ideal tracking and prediction algorithm to solve linear problems. [2]

Estimation in nonlinear systems is crucial, as most real-world systems ranging from engineering to physical processes, exhibit some form of nonlinearity. Two of the most used methods for handling such problems is the Extended Kalman Filter (EKF) and the Unscented Kalman Filter (UKF). The Extended Kalman Filter (EKF) can perform poorly in highly nonlinear systems due to inaccurate linearization, making the Unscented Kalman Filter (UKF) a better choice for more accurate state estimation.

Sonic Booms are the thunder-like noises that originate from aircraft flying at supersonic speeds. A Sonic Boom is formed When the shock waves of the supersonic flow propagate to the ground. Both the creation and the propagation of Sonic Boom are nonlinear phenomena. The minimization of Sonic Boom noise depends on the design of a supersonic aircraft and the selection of the flight conditions in which it will operate. [3]

The goal of our work is to estimate flight conditions and aircraft geometry that produce a desired Sonic Boom signature. This is achieved by developing an algorithm to solve the inverse design problem and achieve low-boom configurations of aircraft geometry and flight conditions. The Unscented Kalman Filter will be used in this algorithm, because the Sonic Boom

Corresponding author: up1061054@ac.upatras.gr

formation is highly nonlinear; unlike the linear Kalman filter it does not assume linearity, and unlike the Extended Kalman Filter it avoids linearization errors by using sigma points to more accurately capture nonlinear state distributions.
The work is organized in two phases. In the first phase, an inverse design algorithm is developed and tested. This algorithm employes an empirical explicit Sonic Boom modeling formula that is not suited for very accurate calculations. Nevertheless, this algorithm can be seen as a proof of concept of applying the (UKF) to a Sonic Boom minimization problem. In the second phase the empirical formula is replaced by a high accuracy nonlinear Sonic Boom formation and propagation model.
In Sec. 2 existing theory about the (UKF) function, the existing empirical model and the more accurate Sonic Boom model is reviewed. In Sec. 3 we proceed with the first phase of proving that an inverse Sonic Boom minimization algorithm is feasible and finally in Sec. 4 a complete inverse aircraft design algorithm for low Boom is presented.

2. Theory

2.1 Unscented Kalman Filter

The Unscented Kalman Filter (UKF) is a nonlinear state-estimation method where uncertain quantities are represented by a state vector X which has a mean value $\hat{X}$ and a covariance P. The UKF also has a measurement vector zk. The UKF represents the state distribution using deterministically selected sigma points. Let n be the number of state variables then the number of sigma points is $2n+1$. The sigma points are distributed around the current state estimate based on the covariance. Specifically, those points are defined as,

$$\begin{aligned} s_0 &= \hat{X},\ s_k = \hat{X} + \left[\sqrt{(n+\lambda)P}\right]_k, \\ s_{k+n} &= \hat{X} - \left[\sqrt{(n+\lambda)P}\right]_k \end{aligned} \quad (1)$$

Each sigma point is passed through a nonlinear mathematical model, $\Upsilon_k = h(s_k)$ and the transformed points are recombined using prescribed weights to approximate the mean and covariance of the predicted output as,

$$\begin{aligned} \hat{z} &= \sum_{k=0}^{2n} W_k^{(m)} \Upsilon_k \\ S_z &= \sum_{k=0}^{2n} W_k^{(c)} \left(\Upsilon_k - \hat{z}\right)\left(\Upsilon_k - \hat{z}\right)^T + R \end{aligned} \quad (2)$$

The relationship between changes in the state variables and changes in the predicted measurements is given by the state–measurement cross covariance,

$$P_{xz} = \sum_{k=0}^{2n} W_k^{(c)} \left(X_k - \hat{x}\right)\left(\Upsilon_k - \hat{z}\right)^T + R \quad (3)$$

The Kalman gain,

$$K = P_{xx} S_z^{-1} \quad (4)$$

determines how strong is the dependance of the state estimate to innovation or in other words it determines the difference between measured and predicted outputs. After an iteration the updated mean and covariance are

$$\begin{aligned} \hat{x}^+ &= \hat{x}^- + K\left(z_k - \hat{z}\right) \\ P^+ &= P^- - K S_z K^T \end{aligned} \quad (5)$$

After updating the mean and covariance a UKF algorithm repeats the process of determining new sigma points until Eq. (5). We can repeat such an update until the measurement vector is sufficiently close to $\hat{z}$.[4]

2.2 Empirical Sonic Boom Formula Carlson-Clare and Oman formula

For the first stage of the work an empirical formula originally presented by Carlson [5] and later refined by Clare and Oman [6] has been used. The formula is based on non-linear fitting on Sonic Boom measurements published in Ref. [7]. For the Boom overpressure the formula found in [6] is employed,

$$\begin{aligned} \Delta p &= 1.075 \cdot K_R \cdot K_A \cdot (M^2-1)^{(1/8)} \cdot H.^{(-3/4)} \cdot P_G \cdot F \\ F &= 0.7437 \cdot \beta + \frac{(3.0201 \cdot W)}{0.5 \gamma P_A M^2 A} + 45.4796 S - 3.1084 \\ S &= 0.4647 b / L - 0.0447 b^2 / A + 0.0001 \cdot \Lambda_E \\ &\quad - 0.0617 F_H / F_L - 0.8598 \cdot A / (L^2) + 0.0599; \end{aligned} \quad (6)$$

where K_R is a ground reflection factor. It was selected equal to 2 for the results presented in this paper assuming acoustically rigid ground. $K_A = \left(P_A / P_G\right)^{1/2}$ is an attenuation factor where P_A is the static pressure at flight altitude and P_G the static pressure at sea level. With M and H we symbolize the flight Mach number and altitude respectively. $\beta = \sqrt{M^2 - 1}$, γ the ratio of specific heats equal to 1.4, and A the wing area of the studied aircraft. S is a shape factor determined by the fuselage height F_H , the fuselage length F_L , the wing sweep angle measured from the leading Edge Λ_E , the wing span b , the total aircraft length L and also by A .
The duration of the Sonic Boom pulse is given by Carlson as,

$$\begin{aligned} \Delta t &= K_t .* (3.42 / c_0) \cdot (M ./ ((M^2-1)^{(3/8)})) \\ &\quad \cdot (H \cdot 0.25) \cdot (L \cdot 0.75) \cdot K_S \end{aligned}, \quad (7)$$

where K_t and K_S are constants determined by graphs in Ref.[5]. and c_0 is the speed of sound at the aircraft altitude.
Those formulas can be used to predict the Sonic Boom overpressure and duration in the basic design

of a supersonic aircraft [3]. Specifically, Clare and Oman report a median absolute relative error overall measurements used to obtain the formulas of 14%. The mean absolute relative error over all measurements was found to be 41.6%. The higher mean error compared to the median is attributed to outliers with very high error.[6].

2.3 Sonic Boom Non-Linear Model

A more accurate physical model was used for the second phase of the work. In this model an F-Witham function is used to determine the near field around the aircraft geometry. The F-function is converted into pressure at 10 aircraft lengths away from the aircraft according to Ref.[8]. The converted pressure signature is propagated to the ground through the atmosphere by solving the non-linear augmented Burgers Equations.

The F- Witham function for the near field is given by,

$$F(x) = \int_0^x \frac{1}{2\pi} \frac{S''_{eq}(u)}{\sqrt{x-u}} du$$
$$S_{Eq}(x) = S_V(x) + S_L(x) \tag{8}$$

where x is the aircraft longitudinal coordinate measured from the aircraft nose. S_{Eq} is an equivalent area that comes from the summation of the cross sections S_V of the aircraft along the Mach angle $\theta = \arcsin(1/M)$ calculated for every x and S_L is an equivalent lift area that comes from the aircraft lift(see jung). In the present work lift area was calculated based on the aircraft assumed weight for simplicity. Better approximations of lift are required for more accurate simulations.

The pressure Δp_A, 10 aircraft lengths away from the aircraft, is given by,

$$\Delta p_A(y) = \frac{\gamma P_A M^2}{20\beta L} F(y).$$
$$y = x - 10\beta L \tag{9}$$

The coordinate y lies on the supersonic flow characteristics. After converting F to pressure y is also converted to time by,

$$\tau = y / c_0 . \tag{10}$$

The resulting waveform $\Delta p_A(\tau)$ is propagated to the ground using an augmented Burgers equations solver. The solver considers the fundamental mechanisms of nonlinear atmospheric pressure wave propagation. Those are: i) geometrical spreading, ii) nonlinear wave distortion, iii) thermoviscous attenuation, iv) molecular relaxation dispersion and v) atmospheric stratification.

The governing equation is,

$$\frac{\partial p}{\partial s} = \frac{\beta_\alpha}{\rho_z c_z^3} p \frac{\partial p}{\partial \tau} + M_{tv}(p) + M_{rel}(p) + M_{geo}(p), \tag{11}$$

where s represents a distance along an acoustic ray and c_z and ρ_z are the ambient speed of sound and ambient air density of the propagation altitude, respectively. $\beta_\alpha = (\gamma+1)/2$ is a non-linear coefficient. The quantities $M_{tv}(p), M_{rel}(p)$, $M_{geo}(p)$, represent the mechanisms of absorption, molecular relaxation, and geometrical spreading, respectively Ref [9].

The initial condition for Eq. (6) is the pressure waveform $\Delta p_A(\tau)$. The propagation of the waveform is not done in a straight line but on acoustic rays which are calculated based on a vertically stratified atmosphere Ref. [10]. Along the propagation the amplitude decreases along the ray due to geometrical spreading. This decrease is given by

$$p / \sqrt{B(s)} \tag{12}$$

where $B(s)$ is the ray bundle area.

The non-linear term $\frac{\partial p}{\partial s} = \frac{\beta_\alpha}{\rho_z c_z^3} p \frac{\partial p}{\partial \tau}$ models the shock creation during the propagation. This equation is solved using a first-order conservative finite-volume Godunov method, and CFL-controlled marching. [See Ref. [9]].

Thermoviscous attenuation and molecular-relaxation effects are evaluated through frequency-dependent atmospheric loss and dispersion models. In the present implementation, these corrections are applied spectrally to the time-domain waveform using FFT and inverse FFT operations, following frequency-domain sonic-boom propagation approaches such as Ref. [11].

Validation of the model was done by comparing its resulting ground Sonic Boom signature to a measured one produced by an F-16 fighter jet flying at 14000ft and 1.1 Mach [7]. Comparisons are shown in Fig. 1(a). The STL geometry of Fig. 1(b) was used for the comparisons. The resulting prediction is reasonably good. The deviation from the experimental data is attributed to the simplified lift calculation used to obtain the equivalent lift area in the F-function.

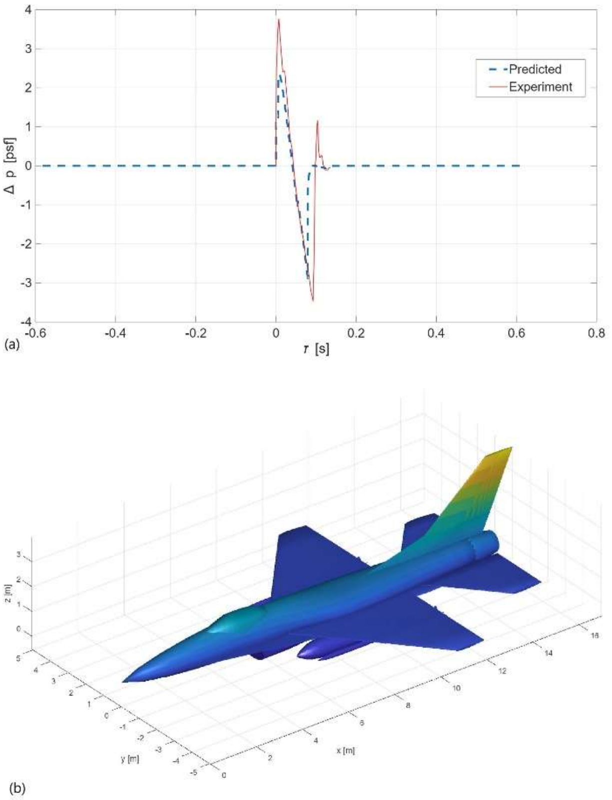

Figure 1. a) Sonic Boom signature produced by an F-16 (solid line) [7] and estimation (dashed line) of that Sonic Boom signature based on the method described in Sec 2.3 and using the simplified geometry of Figure 2 b). b) STL geometry of F-16.

3. Estimation of Mach and Altitude of experimental data using the UKF, and the empirical Formula

In this section we present a method to solve the inverse problem where the input Mach and altitude values need to be found so that the empirical formula produces a pair of measured overpressure and duration. This process is done in order to validate the ability of the UKF to solve the inverse problem. For the purposes of such validation, in order to examine many cases and to avoid complexity, we use the empirical formula presented in Sec. 2. 2 and not the more analytical non-linear propagation solver.

The inversion process is done using the UKF within a simple routine which is described in the following. The measurement vector $z_k = \left[M_{experiment}, H_{experiment} \right]$ contains the target measured overpressure and duration. The state vector x_k contains values of Mach and amplitude. The state vector is initialized as $x_k = x_i = \left[M_i, H_i \right]^T$ and the covariance is initialized as $P = P_i$. The initial sigma points which are 5 are calculated by x_i and P_i as shown in Sec. 2.1. The chosen initial value for covariance is $P_i = \left[0.1^2, 0; 1000^2, 0 \right]$. The selection of the initial value of x_i is more complicated. Some initial values can produce singularities in the application of the filter or lead the algorithm to wrong direction diverging from the desired output. Therefore, we run the routine multiple times and test multiple pairs of initial $\left[M_i, H_i \right]^T$ values. While this approach looks like a brute force search of the desired point it is certainly not. For each initial point the algorithm searches for the solution using the Kalman gain. As a result, this approach is order of magnitudes less costly compared to a brute force search. Specifically, we were able to obtain adequate results using a grid of size 50x50 to pick initial pairs $\left[M_i, H_i \right]^T$. Obtaining similarly accurate results of brute force search would have required grids of far greater size. Also note here, that if accidentally the selected pair was identical or close to the experimental value (i.e. the desired solution) it was rejected from being an initial point.

After the initialization the routine updates the state vector $x_{update} = \left[M_{update}, H_{upadate} \right]$, the covariance P_{update}, and the Sigma Points using the Kalman gain as described in Sec 2.1. The process continues for 20 iterations and the last x_{update} is chosen as the solution of the problem.

Results are shown in Fig. 3 and Fig. 4. Each row in both figures corresponds to different types of aircraft. In the first column of both figures the Mach number M_{update} is compared to the Mach number of the examined measurement $M_{experiment}$ [taken from Ref. [7]], while in the second column H_{update} is compared to $H_{experiment}$ [7]. The third column shows the mean value of the mean relative error between the figures in the same row.

For all aircraft it can be observed that the relative error does not exceed 10% in most cases. Many cases yield very good accuracy close to 5% and there are also some cases when the error can reach 40%. This behavior is expected. Based on theory presented in Sec. 2.2 those errors are very close to the errors reported for the empirical formula.

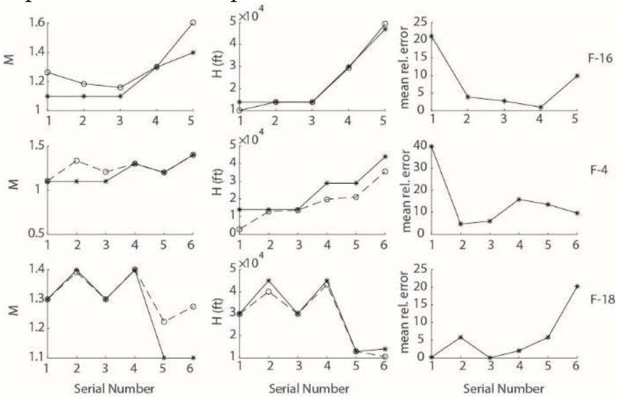

Figure 2. Comparisons between M_{update} (dashed lines open circles) and $M_{experiment}$ [7] (dashed lines filled circles) (first column); comparisons between H_{update} (dashed lines open

circles) and $H_{experiment}$ [7](dashed lines filled circles) (second column); and comparisons between mean of relative errors between the two first columns (third column). First row results for F-16; Second row results for F-4; and third row results for F-18.

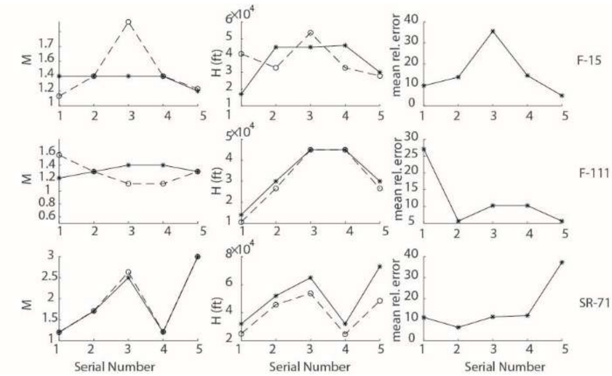

Figure 3. Comparisons between M_{update} (dashed lines open circles) and $M_{experiment}$ [7](dashed lines filled circles) (first column); comparisons between H_{update} (dashed lines open circles) and $H_{experiment}$ [7](dashed lines filled circles) (second column); and comparisons between mean of relative errors between the two first columns (third column). First row results for F-15; Second row results for F-111; and third row results for SR-71.

4. Inverse Design Process

The development of the inverse design process is based on relevant work on Kalman Filter inverse problems found in Refs. [12][13][14].

The goal of the inverse design process is to calculate key geometric and flight characteristics of a simplified supersonic airliner (fuselage and wing only). Specifically, we want to achieve a target value of acoustic annoyance to the ground which is measured in PLdB based on the Stevens Mark VII loudness criterion [15].

For the inverse design process the state vector is,

$$x = \left[M, a, H, A, R_f \right]^T, \tag{13}$$

where a is the angle of attack and R_f the fuselage radius. The values in the x vector may vary within certain ranges depending on the aircraft mission and similar designs. In this work the ranges for all variables are custom selected so that the designed aircraft is a low-boom aircraft of about 60m length and 130000kg weight.

After selecting the ranges of the values of the state vector the algorithm creates simplified aircraft geometries (wing fuselage) by relating the other geometric parameters of the aircraft to randomly picked values of x in the given ranges.

At this point we could select sigma points and for each sigma point and iteration calculate the ground signature based on Sec. 2.3 and the resulting loudness based on Ref.[15]. This process, however, is very expensive due to the complexity of the nonlinear atmospheric propagation model.

As a result, another approach has been followed instead. The ground signature and perceived loudness is calculated using the nonlinear model but only for the aircraft configurations defined earlier. These data are then fitted to create a Gaussian radial-basis surrogate which is way faster than the nonlinear propagation solver. A starting point is then selected from the calculated aircraft and the UKF algorithm as in Sec. 3 is then performed on the surrogate. Then we test whether the resulting aircraft geometry and flight parameters indeed yield the target loudness using the nonlinear model. If the target does not meet the target loudness the process starts again selecting different flight conditions and aircraft geometries as starting points.

The near Field F- functions and the $\Delta p_A(\tau)$ distributions (see Sec. 2.3) are calculated. The $\Delta p_A(\tau)$ distributions are propagated to the ground using the augmented Burgers solver. For each resulting ground signature, the Stevens Mark VII loudness criterion is calculated using a process shown in Ref. [15]

An example of the design process input and output is shown with MATLAB screenshots in Fig. 4 and Fig. 5, respectively. The input includes the ranges of the values of the state vector and the desired range of perceived loudness. The output is the designed aircraft and flight properties and the perceived loudness. The resulting sonic boom ground signature is also shown in Fig. 6

```
% Target loudness interval [PLdB]
targetPLdBRange = [80,90];

% Allowed design ranges
MachRange = [1.30,3];
alphaRange_deg = [-1,4];
altitudeRange_ft = [55000,65000];
wingSurfaceRange_m2 = [150,400];
fuselageRadiusRange_m = [1.20,3.00];
```

Figure 4. Example MATLAB code inverse design algorithm input for the ranges of state vector x_k Eq. (13).

```
========= SST MACH-CUT GROUND BOOM =========
Mach                         = 2.012551
Angle of attack              = 0.815697 deg
Altitude                     = 62190.953 ft
Aircraft length              = 37.175253 m
Wing area                    = 239.930458 m^2
Fuselage radius              = 2.049618 m
Simple CL                    = 0.023459796
Mach-coordinate support      = 38.214365 m
Ground positive peak         = 9.120419 Pa
Ground negative peak         = -14.018726 Pa
Stevens Mark VII loudness    = 89.353124 PLdB
============================================
Final loudness = 89.353124016 PLdB
Target interval = [80.000000000, 90.000000000] PLdB
Target interval reached = 1
========================================================
```

Figure 5. Example MATLAB code inverse design algorithm output.

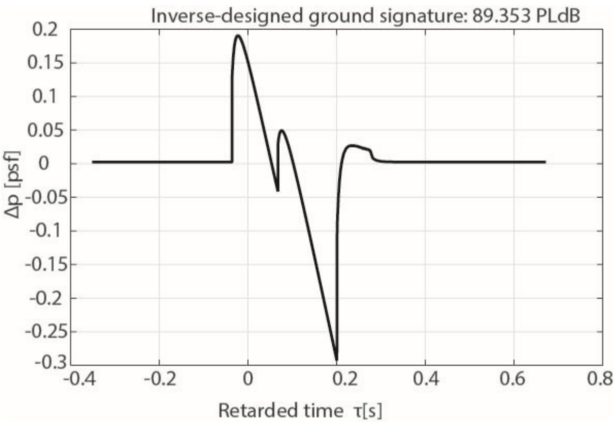

Figure 6. Ground signature produced by the inverse design algorithm that is associated with properties of input from Fig. 4 and output of Fig. 5.

Acknowledgments

This paper has been financed by the funding programme "MEDICUS", of the University of Patras.

References

[1] M. S. Grewal and A. P. Andrews: "Applications of Kalman filtering in aerospace 1960 to the present [Historical Perspectives]," *IEEE Control Systems Magazine*, vol. 30, no. 3, pp. 69–78, 2010. DOI: 10.1109/MCS.2010.936465

[2] R. E. Kalman: "A new approach to linear filtering and prediction problems," Journal of Basic Engineering, vol. 82, no. 1, pp. 35–45, 1960.

[3] G. Bonavolontà, C. Lawson, and A. Riaz: "Review of sonic boom prediction and reduction methods for next generation of supersonic aircraft," Aerospace, vol. 10, no. 11, article 917, 2023.

[4] S. J. Julier and J. K. Uhlmann: "Unscented filtering and nonlinear estimation," Proceedings of the IEEE, vol. 92, no. 3, pp. 401–422, 2004.

[5] H. W. Carlson: Simplified Sonic-Boom Prediction. NASA Technical Paper 1122, National Aeronautics and Space Administration, 1978.

[6] A. Clare and R. Oman, "Sonic boom prediction: A new empirical formulation and animated graphical model," in Proc. of Transformational Science and Technology for the Current and Future Force, pp. 565–572, 2006.

[7] R. A. Lee and J. M. Downing: Sonic Booms Produced by United States Air Force and United States Navy Aircraft: Measured Data. Final Report AL-TR-1991-0099, Armstrong Laboratory, Wright-Patterson Air Force Base, OH, 1991

[8] T. P. Jung: Modified Linear Theory Aircraft Design Tools and Sonic Boom Minimization Strategy Applied to Signature Freezing via F-Function Lobe Balancing. Ph.D. dissertation, University of Colorado at Boulder, Boulder, CO, USA, 2012.

[9] S. K. Rallabhandi, M. Nemec, and M. J. Aftosmis, "Recent enhancements to modeling sonic boom propagation using augmented Burgers' equation," in Proc. of the AIAA Aviation 2023 Forum, paper AIAA 2023-3727, 2023.

[10] R. O. Cleveland: Propagation of Sonic Booms through a Real, Stratified Atmosphere. Ph.D. dissertation, The University of Texas at Austin, Austin, TX, USA, 1995.

[11] S. K. Rallabhandi and D. N. Mavris, "Design and analysis of supersonic business jet concepts," in Proc. of the 6th AIAA Aviation Technology, Integration and Operations Conference (ATIO), Wichita, KS, USA, paper AIAA 2006-7702, 2006.

[12] D. Z. Huang, T. Schneider, and A. M. Stuart: "Iterated Kalman methodology for inverse problems," Journal of Computational Physics, vol. 463, article 111262, 2022.

[13] R. G. Regis and C. A. Shoemaker: "Constrained global optimization of expensive black box functions using radial basis functions," Journal of Global Optimization, vol. 31, no. 1, pp. 153–171, 2005.

[14] M. D. McKay, R. J. Beckman, and W. J. Conover: "A comparison of three methods for selecting values of input variables in the analysis of output from a computer code," Technometrics, vol. 21, no. 2, pp. 239–245, 1979.

[15] S. S. Stevens: "Perceived level of noise by Mark VII and decibels (E)," The Journal of the Acoustical Society of America, vol. 51, no. 2B, pp. 575–601, 1972.